A Derivative-Free Observability Analysis Method of Stochastic Power Systems

Zongsheng Zheng, *Member, IEEE*, Yijun Xu, *Member, IEEE*, Lamine Mili, *Life Fellow, IEEE*, Zhigang Liu, *Senior Member, IEEE*, Mert Korkali, *Senior Member, IEEE*, Yuhong Wang, *Member, IEEE*

***Abstract*—The observability analysis of a time-varying nonlinear dynamic model has recently attracted the attention of power engineers due to its vital role in power system dynamic state estimation. Generally speaking, due to the nonlinearity of the power system dynamic model, the traditional derivative-based observability analysis approaches either rely on the linear approximation to simplify the problem or require a complicated derivation procedure that ignores the uncertainties of the dynamic system model and of the observations represented by stochastic noises. Facing this challenge, we propose a novel polynomial-chaos-based *derivative-free* observability analysis approach that not only brings a low complexity, but also enables us to quantify the degree of observability by considering the stochastic nature of the dynamic systems. The excellent performances of the proposed method is demonstrated using simulations of a decentralized dynamic state estimation performed on a power system using a synchronous generator model with IEEE-DC1A exciter and a TGOV1 turbine-governor.**

***Index Terms*—Dynamic state estimation, observability analysis, derivative-free analysis, polynomial chaos.**

I. Introduction

Dynamic state estimation (DSE) is an important technique in modern power systems, and it is used for obtaining the dynamic state variables in a timely and an accurate manner. The real-time information of the dynamic states is crucial for various devices to enhance system security and stability [1].

To properly design and implement such a dynamic state estimator of a system, observability analysis is a prerequisite. Traditionally, the convential observability analysis of a nonlinear power system dynamic model relies on the small-signal approximation of the system model. Although this method is simple, an inaccurate or even incorrect result can be obtained under a highly nonlinear condition. Therefore, some alternative approaches are proposed to address this issues. Qi *et al.* [2] adopt the empirical observability Gramian to enhance the Phasor Measurement Unit (PMU) placement to achieve system observability. Although being a computable tool, the approximated constant impedance load models can reduce the accuracy of the analysis result. Recently, the Lie derivatives are advocated for the observability analysis of power system dynamic states. For instance, in [3], the Lie-derivative-based observability analysis approach is utilized to evaluate the observability of several test systems where the synchronous generators are represented by the classical model. This work is further extended in [4]. Albeit accurate under a nonlinear condition, this approach is known to be derivative-complicated and very time-consuming even for small-scale power systems. Finally, we would like to emphasize that none of the above observability methods accounts for the intrinsic stochasticity of the dynamic model of the system.

To address the above issues, we propose a novel polynomial-chaos-based approach that enables the observability analysis for the decentralized power system dynamical state estimation, yielding the following contributions: (1) Unlike the traditional linear-approximation-based method, the proposed method is based on the polynomial-chaos theory that has no linear assumption. In contrast to the derivative-complicated Lie derivative method, the proposed approach is fully *derivative-free*, which greatly reduces the derivative complexity and computational burden. (2) Power systems are intrinsically stochastic while the traditional observability analysis methods are within a deterministic scope. To account for the system randomness in the observability analysis and to better describe the degree of the system observability, we further develop the index of the *puny* and *brawny* observability by which the proposed approach can not only analyze the observability of each system state, but can also assess the effect of the dynamic system model and observation noise on the system observability. (3) Finally, since the decentralized DSE is advocated more often than the centralized DSE in the literature for its capability of eliminating the uncertainties of the line and transformer models and the loads within a centralized system model [1], [5], [6], we merge the proposed method into the decentralized DSE framework to ensure a better practical observability analysis. Using the above strategies, the simulations conducted on a decentralized power system dynamic state estimator reveal the excellent performances of the proposed method.

II. Observability Analysis in Power System Dynamic Model

Here, let us first review of the observability analysis for a time-varying dynamic system. Then, we will extend it to the case of a decentralized power system dynamic model.

1) Review of Observability: Consider a general discrete-time dynamical system formulated as

$$\boldsymbol{x}_{k+1} = \boldsymbol{f}(\boldsymbol{x}_k), \boldsymbol{y}_k = \boldsymbol{h}(\boldsymbol{x}_k), \tag{1}$$

This work was supported, in part, by the U.S. NSF Grant 1917308 and by the U.S. DOE Office of Electricity Advanced Grid Modeling Program, and performed under the auspices of the U.S. DOE by LLNL under Contract DE-AC52-07NA27344. Document released as LLNL-CONF-816401.

Z. Zheng, Y. Xu, and L. Mili are with the Bradley Department of Electrical and Computer Engineering, Virginia Tech, Northern Virginia Center, Falls Church, VA 22043 USA (e-mail:{zongsheng, yijunxu, lmili}@vt.edu).

Z. Liu is with the School of Electrical Engineering, Southwest Jiaotong University, Chengdu, 610031 China (e-mail: liuzg_cd@126.com).

M. Korkali is with the Lawrence Livermore National Laboratory, Livermore, CA 94550 USA (e-mail: korkali1@llnl.gov).

Y. Wang is with the College of Electrical Engineering, Sichuan University, Chengdu, 610065 China (e-mail: yuhongwang@scu.edu.cn).

978-1-6654-0507-2/21/$31.00 ©2021 IEEE

where $\boldsymbol{x}_k \in \mathbb{R}^{n\times 1}$ and $\boldsymbol{y}_k \in \mathbb{R}^{m\times 1}$ are the state and the measurement vectors at time k, respectively; and $\boldsymbol{f}$ and $\boldsymbol{h}$ are vector-valued functions.

Definition 1: The system is (locally) observable in the time interval $[0, K]$ if the initial state $\boldsymbol{x}_0$ can be uniquely determined from $\boldsymbol{y}_k$, $k \in [0, K]$.

Defining the cumulative measurement vector $\mathcal{Y}_k = [\boldsymbol{y}_k, \boldsymbol{y}_{k+1}, \ldots, \boldsymbol{y}_{k+n-1}]^\mathsf{T}$, the relation between the arbitrary initial state $\boldsymbol{x}_k$ and its corresponding measurements $\mathcal{Y}_k$ is given by

$$\mathcal{Y}_k = \boldsymbol{g}(\boldsymbol{x}_k). \tag{2}$$

According to the implicit function theorem, the initial state $\boldsymbol{x}_k$ can be uniquely determined from the measurements $\mathcal{Y}_k$ if and only if the Jacobian matrix

$$\boldsymbol{O}_k = \frac{\partial \mathcal{Y}_k}{\partial \boldsymbol{x}_k} \tag{3}$$

is nonsingular. Consequently, the observability rank condition is described as follows:

Theorem 1: The system (1) is (locally) observable if and only if the Jacobian matrix (also called observability matrix) has full rank, i.e., $\mathrm{rank}(\boldsymbol{O}_k) = n$.

Its state-measurement relation (2) can be represented by

$$\mathcal{Y}_k = [\boldsymbol{h}(\boldsymbol{x}_k), \boldsymbol{h}(\boldsymbol{f}(\boldsymbol{x}_k)), \boldsymbol{h}(\boldsymbol{f}(\boldsymbol{f}(\boldsymbol{x}_k))), \cdots]^\mathsf{T}, \tag{4}$$

and the corresponding observability is computed through

$$\boldsymbol{O}_k = \left[\frac{\partial \boldsymbol{h}(\boldsymbol{x}_k)}{\partial \boldsymbol{x}_k}, \frac{\partial \boldsymbol{h}(\boldsymbol{f}(\boldsymbol{x}_k))}{\partial \boldsymbol{x}_k}, \frac{\partial \boldsymbol{h}(\boldsymbol{f}(\boldsymbol{f}(\boldsymbol{x}_k)))}{\partial \boldsymbol{x}_k}, \cdots\right]^\mathsf{T}. \tag{5}$$

As (5) has shown, the derivation procedure for the observability matrix can be complicated for nonlinear and high-dimensional dynamic systems. This is especially true for power systems as shown in [4]. This motivates us to propose a derivative-free approach to simplify this procedure.

2) Power System Dynamics: Here, to represent the power system dynamic model, $\boldsymbol{x}_{k+1} = \boldsymbol{f}(\boldsymbol{x}_k)$, the synchronous generator with a IEEE-DC1A exciter and a TGOV1 turbine-governor is selected and modeled as

$$T'_{d_0}\frac{\mathrm{d}E'_q}{\mathrm{d}t} = -E'_q - (X_d - X'_d)I_d + E_{fd}, \tag{6}$$

$$T'_{q_0}\frac{\mathrm{d}E'_d}{\mathrm{d}t} = -E'_d - (X_q - X'_q)I_q, \tag{7}$$

$$\frac{\mathrm{d}\delta}{\mathrm{d}t} = \omega - \omega_s, \tag{8}$$

$$\frac{2H}{\omega_s}\frac{\mathrm{d}\omega}{\mathrm{d}t} = T_M - P_e - D(\omega - \omega_s), \tag{9}$$

$$T_E\frac{\mathrm{d}E_{fd}}{\mathrm{d}t} = -(K_E + S_E(E_{fd}))E_{fd} + V_R, \tag{10}$$

$$T_F\frac{\mathrm{d}V_F}{\mathrm{d}t} = -V_F + \frac{K_F}{T_E}V_R - \frac{K_F}{T_E}(K_E + S_E(E_{fd}))E_{fd}, \tag{11}$$

$$T_A\frac{\mathrm{d}V_R}{\mathrm{d}t} = -V_R + K_A(V_{\mathrm{ref}} - V_F - V), \tag{12}$$

$$T_{CH}\frac{\mathrm{d}T_M}{\mathrm{d}t} = -T_M + P_{SV}, \tag{13}$$

$$T_{SV}\frac{\mathrm{d}P_{SV}}{\mathrm{d}t} = -P_{SV} + P_C - \frac{1}{R_D}(\frac{\omega}{\omega_s} - 1), \tag{14}$$

where δ and ω are generator rotor angle and speed, respectively; ω_s is the rotor speed base value; T'_{d_0}, T'_{q_0}, T_E, T_F, T_A, T_{CH}, and T_{SV} are the time constants; K_E, K_F, and K_A are the controller gains; E'_d, E'_q, E_{fd}, V_F, V_R, T_M, and P_{SV} are the d- and q-axis transient voltages, field voltage, scaled output of the stabilizing transformer and scaled output of the amplifier, synchronous machine mechanical torque and steam valve position, respectively; X_d, X'_d, X_q, and X'_q are the generator parameters; H, D, and R_D are the inertia constant (in seconds), damping ratio and droop, respectively; V_{ref} and P_C are the known references for exciter and speed governor, respectively; V and θ are the terminal bus voltage magnitude and phase angle, respectively.

3) Decentralized Generator Model: The decentralized synchronous generator model along with the associated measurement model and the notations are following Zhao and Mili [7]. Here, when a disturbance occurs in the system, the local PMU of the ith generator records the output voltage phasor, $V_i\angle\theta_i$, and the output current phasor, $I_i\angle\phi_i$, yielding $V_{di} = V_i\sin(\delta_i - \theta_i)$, $V_{qi} = V_i\cos(\delta_i - \theta_i)$, $I_{di} = (E'_{qi} - V_{qi})/X'_{di}$ and $I_{qi} = (V_{di} - E'_{di})/X'_{qi}$. This enables us to calculate the active power and reactive power for the ith generator as model outputs, which are expressed as

$$P_{ei} = V_{di}I_{di} + V_{qi}I_{qi} + e_{Pi}, \tag{15}$$

$$Q_{ei} = -V_{di}I_{qi} + V_{qi}I_{di} + e_{Qi}, \tag{16}$$

where e_{Pi} and e_{Qi} are the measurement noise. By this way, once we capture the local voltage phasor $V_i\angle\theta_i$ as the play-in function, which is proposed in [5], the play-out function, namely P_{ei} and Q_{ei}, can be simulated through its corresponding system and measurement model as described by (6)-(16). This is the decentralized generator model used in this paper. More details can be referred to [7].

III. Polynomial-Chaos-based Observability Analysis Approach

Before we present the generalized-polynomial-chaos(gPC)-based observability analysis, let us have a brief review of the gPC theory first.

A. Review of the Generalized Polynomial Chaos

1) gPC surrogate: The gPC, which is first introduced by Wiener and further developed by Xiu and Karniadakis [8], has been demonstrated to be a cost-effective tool in uncertainty propagation of a linear or nonlinear system model [8], [9]. In this theory, the stochastic outputs are expressed as a weighted sum of orthogonal polynomial chaos basis functions constructed from the probability distribution of the random variables, i.e.,

$$y = \sum_{i=0}^{n_p} a_i\phi_i(\boldsymbol{\xi}), \tag{17}$$

where y is the system out, $\boldsymbol{\xi} = [\xi_1, \xi_2, \ldots, \xi_n]$ is a vector of random variables following a standard probability distribution, and its corresponding polynomial chaos basis is $\phi_i(\boldsymbol{\xi})$, a_i is the ith polynomial chaos coefficient, $n_p = (n+p)!/(n!p!) - 1$, and p is the maximum order of the polynomial chaos basis functions. From the polynomial chaos coefficients, the mean and the variance of the output y can be directly obtained as

$$\mu = a_0, \sigma^2 = \sum_{i=1}^{n_p} a_i^2. \tag{18}$$

In practice, to maintain the computational efficiency of the surrogate model, (17), a truncated PCE is typically adopted. Although different truncation strategies exist, considering the scalability and accuracy of the power system model, we propose to select the strategy proposed in [10] to truncate the gPC surrogate as

$$y = a_0\phi_0 + \sum_{i=1}^{n} a_i\phi_1(\xi_i) + \sum_{i=1}^{n} a_{i,i}\phi_2(\xi_i^2), \tag{19}$$

where $\phi_0, \phi_1(\xi_i), \phi_2(\xi_i^2)$ represent the zero-, first-, second-order polynomial chaos bases; and $a_0, a_i, a_{i,i}$ stand for the corresponding polynomial chaos coefficients.

2) Collocation Points: Collocation points (CPs) are a finite sample set of $\boldsymbol{\xi} = [\xi_1, \xi_2, \ldots, \xi_n]$ that are chosen to approximate the polynomial chaos coefficients. The elements of the CPs are generated by using the union of the zeros and the roots of one higher-order, one-dimensional polynomial for every random variable. Then, using a tensor product or sparse tensor rule, we can generate multidimensional CPs as described in [8], [10]. Here, for Gaussian random variables, Hermite polynomials are selected.

3) Approximation of gPC Coefficients: Here, let us present the way to approximate the gPC coefficients for a general function

$$\boldsymbol{y} = \boldsymbol{g}(\boldsymbol{x}) \tag{20}$$

where the input variable is $\boldsymbol{x} \in \mathbb{R}^{n\times 1}$, and the output variable is $\boldsymbol{y} \in \mathbb{R}^{L\times 1}$. To achieve the surrogate model, the coefficients of gPC are estimated at selected combinations of the aforementioned collocation points, $\boldsymbol{\xi}$. Taking into consideration S independent combinations of the collocation points, the polynomial chaos basis can be obtained directly, and the output variable can be calculated through the considered function (20). Formally, the surrogate model is given by

$$\boldsymbol{Y} = \boldsymbol{H}\boldsymbol{A}, \tag{21}$$

where $\boldsymbol{Y} \in \mathbb{R}^{S\times L}$ is the output matrix consisting of the outputs from S samples; $\boldsymbol{H} \in \mathbb{R}^{S\times(2n+1)}$ is the basis matrix composed of the polynomial chaos bases expressed as

$$\boldsymbol{H} = \begin{bmatrix} \phi_0 & \phi_1(\xi_{1,1}) & \cdots & \phi_1(\xi_{1,n}) & \phi_2(\xi_{1,1}^2) & \cdots & \phi_2(\xi_{1,n}^2) \\ \phi_0 & \phi_1(\xi_{2,1}) & \cdots & \phi_1(\xi_{2,n}) & \phi_2(\xi_{2,1}^2) & \cdots & \phi_2(\xi_{2,n}^2) \\ \vdots & \vdots & \vdots & \vdots & \vdots & \ddots & \vdots \\ \phi_0 & \phi_1(\xi_{S,1}) & \cdots & \phi_1(\xi_{S,n}) & \phi_2(\xi_{S,1}^2) & \cdots & \phi_2(\xi_{S,n}^2) \end{bmatrix} \tag{22}$$

and $\xi_{s,i}$ is the ith element of the sth sample; $A \in \mathbb{R}^{(2n+1)\times L}$ is the coefficient matrix

$$\boldsymbol{A} = \begin{bmatrix} a_0^{(1)} & a_0^{(2)} & \cdots & a_0^{(L)} \\ a_1^{(1)} & a_1^{(2)} & \cdots & a_1^{(L)} \\ \vdots & \vdots & \ddots & \vdots \\ a_n^{(1)} & a_n^{(2)} & \cdots & a_n^{(L)} \\ a_{1,1}^{(1)} & a_{1,1}^{(2)} & \cdots & a_{1,1}^{(L)} \\ \vdots & \vdots & \ddots & \vdots \\ a_{n,n}^{(1)} & a_{n,n}^{(2)} & \cdots & a_{n,n}^{(L)} \end{bmatrix}, \tag{23}$$

and $a_0^{(l)}, a_i^{(l)}, a_{i,i}^{(l)}$ stand for the polynomial chaos coefficients with respect to the ith input and lth output.

Based on the obtained basis and output matrices, the coefficient matrix can be calculated through

$$\boldsymbol{A} = \boldsymbol{H}^{-1}\boldsymbol{Y}. \tag{24}$$

According to (18), the mean of the output variable is $\hat{\boldsymbol{y}} = \boldsymbol{A}_1 = [a_0^{(1)}, a_0^{(2)}, \cdots, a_0^{(L)}]^{\intercal}$, and the covariance matrix of the output variable is given by $\boldsymbol{P}_y = \boldsymbol{A}_2^{\intercal}\boldsymbol{A}_2$, where $\boldsymbol{A}_2$ is the rest $2n\times L$ matrix of $\boldsymbol{A}$, reflecting the second-moment information.

B. The Proposed gPC-based Observability Analysis Approach

In the traditional approach, multiple derivatives are involved in the calculation of the observability matrix, which leads to a heavy computational burden. To achieve a lower computational burden and account for the stochasticity of the system, a derivative-free approach based on the gPC is proposed.

Since we are considering a more general stochastic dynamic system instead of the traditional deterministic system in (1), let us extend the concept for the observability to a stochastic dynamic system as follows:

Definition 2: A stochastic system is (locally) observable in the time interval $[0, K]$ if the initial state $\boldsymbol{x}_0$ can be inferred from the measurements $\boldsymbol{y}_k$, $k \in [0, K]$ and its solution satisfies a certain confidence interval level.

Consider the discrete-time dynamical system (1). Instead of the original response function (2), we use a surrogate model to represent the relation between the arbitrary initial state $\boldsymbol{x}_k$ and its corresponding measurements $\mathcal{Y}_k$ as

$$\boldsymbol{Y}_k = \boldsymbol{H}\boldsymbol{A}_k. \tag{25}$$

In the surrogate model, since the means of the first-order and second-order polynomial chaos bases are zeros due to the orthogonal property [8], the zero-order polynomial chaos basis and its corresponding polynomial chaos coefficient $(a_0^{(l)}\phi_0)$ denotes the mean of the lth measurement, and the first-order and the second-order polynomial chaos bases and their corresponding polynomial chaos coefficients $(a_i^{(l)}\phi_1(\xi_{s,i})$ and $a_{i,i}^{(l)}\phi_2(\xi_{s,i}^2))$ represent the uncertainty of the lth measurement with respect to the uncertainty of the ith state, where $\phi_1(\xi_{s,i})$ and $\phi_2(\xi_{s,i}^2)$ denotes the first-order and second-order polynomial chaos bases associated with the ith state. Further, the polynomial chaos coefficients, $a_i^{(l)}$ and $a_{i,i}^{(l)}$, stand for the contribution of the ith state to the uncertainty of the lth measurement.

When the contribution of the ith state to the uncertainty of the lth measurement is zero, it means the value of the lth measurement remains unchanged with respect to the variations in this state, that is, the ith state can not be inferred from the lth measurement. To infer the n states from the given measurements uniquely, n effective measurements are needed, for which the contributions of the states to the uncertainties of the measurements are linearly independent. That is, the observability-coefficient matrix $\boldsymbol{\Phi}_k \in \mathbb{R}^{2n\times mn}$

$$\boldsymbol{\Phi}_k = \begin{bmatrix} a_1^{(1)} & a_1^{(2)} & \cdots & a_1^{(mn)} \\ \vdots & \vdots & \ddots & \vdots \\ a_n^{(1)} & a_n^{(2)} & \cdots & a_n^{(mn)} \\ a_{1,1}^{(1)} & a_{1,1}^{(2)} & \cdots & a_{1,1}^{(mn)} \\ \vdots & \vdots & \ddots & \vdots \\ a_{n,n}^{(1)} & a_{n,n}^{(2)} & \cdots & a_{n,n}^{(mn)} \end{bmatrix}, \tag{26}$$

which is the submatrix of the coefficient matrix, has n linearly independent columns, and the ith and $(n+i)$th rows cannot be zeros.

Theorem 2: The system (1) is (locally) observable if and only if the observability-coefficient matrix $\boldsymbol{\Phi}_k$ has n linearly independent columns and the ith and $(n+i)$th rows cannot be all zeros.

C. Degree of Observability

Since the extended definition of the observability of a stochastic dynamic system introduced in *Definition 2* also focuses on the confidence of the solution, we would like to further propose two new quantitative observability indices to measure the degree of observability from three aspects.

1) Contribution Rate: According to the surrogate model, the variance of the lth measurement can be determined via

$$\sigma_y^{2(l)} = \sum_{i=1}^{n} a_i^{2(l)} + a_{i,i}^{2(l)}, \tag{27}$$

where $\{a_i^{2(l)} + a_{i,i}^{2(l)}\}$ denotes the contribution of the ith state to the variance of the lth measurement.

Define the proportion of the contribution of the ith state to the variance of the lth measurement as the contribution rate, i.e.,

$$Q_i^{(l)} = \frac{a_i^{2(l)} + a_{i,i}^{2(l)}}{\sigma_y^{2(l)}}. \tag{28}$$

It follows that $0 \leq Q_i^{(l)} \leq 1$. The contribution rate denotes the influence of the state on the measurement. A larger contribution rate means a larger influence of the state on the measurement, and vice versa.

Definition 3: if all the contribution rates $(Q_i^{(1)}, Q_i^{(2)}, \ldots, Q_i^{(mn)})$ of the ith state are less than a small positive value (e.g., 0.1%), that state is *puny* observable. Otherwise, it is brawny observable. If all the states are *brawny* observable, the system is brawny observable. Otherwise, the system is puny observable. ■

2) Numerical Stability: To guarantee the numerical stability of the estimated state, the observability-coefficient matrix must be well-conditioned. The condition number, which is the ratio of the largest singular value to the smallest one

$$c(\mathbf{\Phi}) = \frac{\sigma_{\max}(\mathbf{\Phi})}{\sigma_{\min}(\mathbf{\Phi})} \tag{29}$$

is used to evaluate the matrix.

Definition 4: If the condition number is very large or becomes infinity, the system is puny observable. If the condition number is close to one, the system is brawny observable. ■

3) Interference Rate: Our approach can also assess the effect of observation noise on system observability.

If the contribution of the ith state given by $a_i^{2(l)} + a_{i,i}^{2(l)}$ to the variance of the lth measurement is close or smaller than the measurement noise variance $\sigma_v^{2(l)}$, its influence is difficult to distinguish from that of the noise variance.

Define the proportion of the noise variance to the variance of the lth measurement as the interference rate, i.e.,

$$V^{(l)} = \frac{\sigma_v^{2(l)}}{\sigma_z^{2(l)}}. \tag{30}$$

Definition 5: For a noisy measurement environment, the ith state is puny observable when all the contribution rates $(Q_i^{(1)}, Q_i^{(2)}, \ldots, Q_i^{(mn)})$ are less than the corresponding interference rates $(V^{(1)}, V^{(2)}, \ldots, V^{(mn)})$. ■

IV. Simulation Results

In this section, the observability analysis for power system dynamic state estimation is performed by using our approach. As a benchmark system, the IEEE 10-machine, 39-bus system is considered, and the synchronous generator is modeled by a ninth-order two-axis model with a IEEE-DC1A exciter and a TGOV1 turbine-governor. The decentralized dynamic state estimation is implemented, in which the real and reactive power injections and the bus voltage phasors are assumed to be metered using PMUs. The PMU measurements are assumed to be received at a rate of 60 samples per second. A disturbance is applied at $t = 0.5$ s by opening the transmission line between Buses 19 and 33.

Consider a general case, in which both the real and reactive power are used as measurements for state estimation. In the observability-coefficient matrix, the first-order polynomial chaos coefficients are much larger than the second-order polynomial chaos coefficients. For the convenience of illustration, we define a matrix composed of the first-order polynomial chaos coefficients (i.e., the first n rows of the observability-coefficient matrix) and call it the *first-order* coefficient matrix.

The observability condition is tested first, and the rank of the observability-coefficient matrix is shown in Fig. 1(a). It is shown that the observability-coefficient matrix cannot be full rank at all the time. However, as shown in Fig. 1(b), the first-order coefficient matrix has full rank at all the time, which satisfies the observability condition. Hence, the system is obse

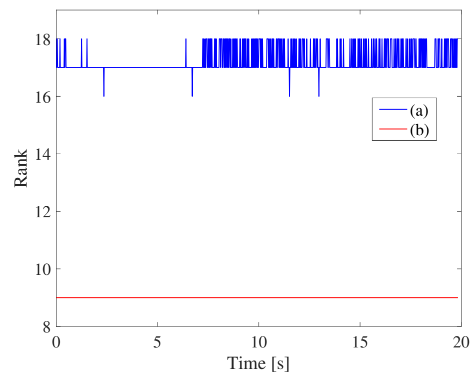

Fig. 1. Rank of the matrices. (a) the observability-coefficient matrix, (b) the first-order coefficient matrix.

Next, the degree of observability is discussed. The contribution rate is considered first, and the maximum contribution rate is shown in Fig. 2. As can be seen, the first four states have the larger contribution rates, which means they can estimated with the given measurements. Note that the other five states have negligible contribution rates, which means it is hard for them to be inferred from the given measurements. That is to say, the first four states are brawny observable while the other five states are puny observable.

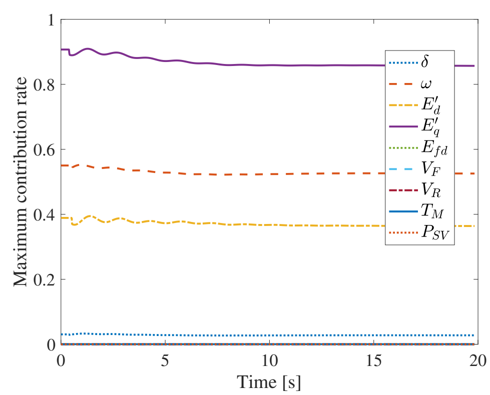

Fig. 2. Maximum contribution rate.

Since the rank of the observability-coefficient matrix cannot be full rank all the time, the condition number of the observability-coefficient matrix can sometimes be very large. The condition number of the first-order coefficient matrix is demonstrated in Fig. 3(a). The condition number of the first-order coefficient matrix varies with time while taking large values that result in ill-conditioned observability matrix. Consequently, the state estimate is not numerically stable, which is in agreement with the result obtained from the contribution rate. For the convenience of illustration, we define a matrix composed of the first four rows of the first-order coefficient matrix, which correspond to the first four states with brawny observability, and call it the *first-four* coefficient matrix. The condition number of the first-four coefficient matrix is demonstrated in Fig. 3(b). It shows that the condition number of the first-four coefficient matrix is small enough to ensure that the first-four coefficient matrix is well-conditioned, which means the first-four states can be well estimated.

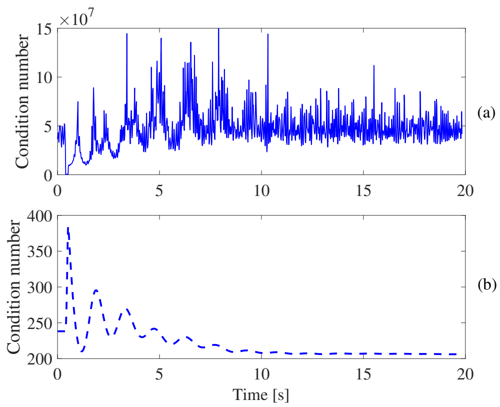

Fig. 3. Condition number of the matrices: (a) the first-order coefficient matrix and (b) the first-four coefficient matrix.

Finally, the effect of the observation noise on the observability of the dynamical system is discussed. The interference rate is considered, and the maximum interference rate is shown in Fig. 4. As can be seen, the maximum interference rate is very small, which has negligible effect on the measurement. Hence, the effect of the observation noise on the state estimation is negligible.

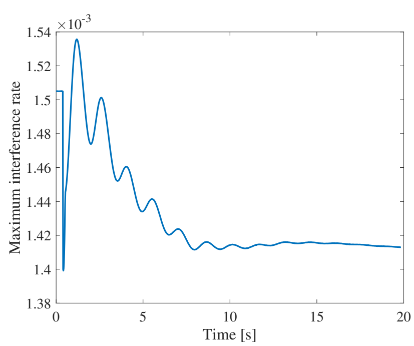

Fig. 4. Maximum interference rate.

The effectiveness of the observability analysis result is verified through power system dynamic state estimation by using the polynomial-chaos-based Kalman filter (PCKF) [10]. As examples, four states are demonstrated in Fig. 5. Two types of implementation are considered. One performs the state estimation with the complete state propagation and the state correction, as shown in Fig. 5(a). In the other implementation, the state correction of the last five states with puny observability is canceled, as shown in Fig. 5(b). As can be seen, the state estimation results obtained from both implementations are the same, and they match very well the true states. In this case, although the last five states are puny observable (i.e., they are hard to be inferred from the measurements), they can be estimated through the state propagation with good state initiation.

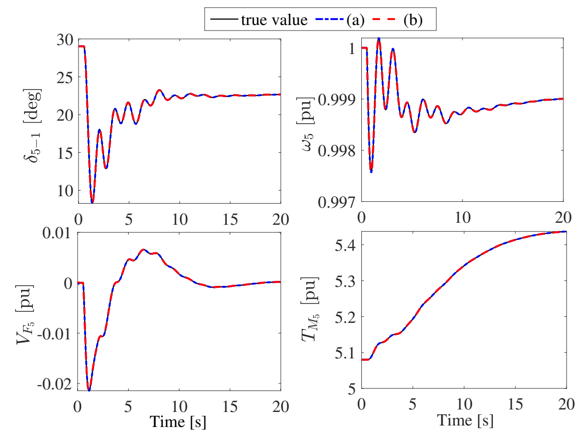

Fig. 5. Case 1: State estimation results. (a) the state estimation is performed with the complete state propagation and the state correction, (b) the state correction of the last five states is canceled.

V. Conclusions

In this paper, we propose a novel polynomial-chaos-based derivative-free observability analysis approach for power system dynamic model. This method not only has a low complexity and an easy implementation, but also enables us to quantify the degree of observability. The excellent performances of the proposed method have been revealed in the simulations for the power system decentralized DSE.

References

[1] J. Zhao *et al.*, "Power system dynamic state estimation: motivations, definitions, methodologies and future work," *IEEE Trans. Power Syst.*, vol. 34, no. 4, pp. 3188–3198, Jul. 2019.

[2] J. Qi, K. Sun, and W. Kang, "Optimal PMU placement for power system dynamic state estimation by using empirical observability gramian," *IEEE Trans. Power Syst.*, vol. 30, no. 4, pp. 2041–2054, Jul. 2015.

[3] G. Wang, C. Liu, N. Bhatt, E. Farantatos, and M. Patel, "Observability of nonlinear power system dynamics using synchrophasor data," *Int. Trans. Electr. Energy Syst.*, vol. 26, no. 5, pp. 952–967, May 2016.

[4] A. Rouhani and A. Abur, "Observability analysis for dynamic state estimation of synchronous machines," *IEEE Trans. Power Syst.*, vol. 32, no. 4, pp. 3168–3175, Jul. 2017.

[5] Z. Huang, P. Du, D. Kosterev, and S. Yang, "Generator dynamic model validation and parameter calibration using phasor measurements at the point of connection," *IEEE Trans. Power Syst.*, vol. 28, no. 2, pp. 1939–1949, May 2013.

[6] A. K. Singh and B. C. Pal, "Decentralized dynamic state estimation in power systems using unscented transformation," *IEEE Trans. Power Syst.*, vol. 29, no. 2, pp. 794–804, Mar. 2014.

[7] J. Zhao and L. Mili, "Power system robust decentralized dynamic state estimation based on multiple hypothesis testing," *IEEE Trans. Power Syst.*, vol. 33, no. 4, pp. 4553–4562, Jul. 2018.

[8] D. Xiu and G. E. Karniadakis, "The Wiener–Askey polynomial chaos for stochastic differential equations," *SIAM J. Sci. Comput.*, vol. 24, no. 2, pp. 619–644, 2002.

[9] Y. Xu, L. Mili, A. Sandu, M. R. von Spakovsky, and J. Zhao, "Propagating uncertainty in power system dynamic simulations using polynomial chaos," *IEEE Trans. Power Syst.*, vol. 34, no. 1, pp. 338–348, Jan. 2019.

[10] Y. Xu, L. Mili, and J. Zhao, "A novel polynomial-chaos-based Kalman filter," *IEEE Signal Process. Lett.*, vol. 26, no. 1, pp. 9–13, Jan. 2019.